Eur. Phys. J. A (2015) **51**: 151
DOI 10.1140/epja/i2015-15151-7

THE EUROPEAN PHYSICAL JOURNAL A

Regular Article – Theoretical Physics

Nature of $K^\pi = 0_2^+$ bands in A = 140–180 region, a global analysis

J.B. Gupta[1,a] and J.H. Hamilton[2]

[1] Ramjas College, University of Delhi, Delhi-110007, India
[2] Physics Department, Vanderbilt University, Nashville, TN, 37235 USA

Received: 11 July 2015 / Revised: 25 September 2015
Published online: 25 November 2015 – © Società Italiana di Fisica / Springer-Verlag 2015
Communicated by A. Ramos

Abstract. The nature of $K^\pi = 0_2{}^+$ band is analyzed in the light of the variation of the $E(0_2{}^+)$ and $B(E2)$ values, with N and Z, for the $A = 140$–180 region. The absolute $B(E2)$ strengths for the excitation of 2_γ and $2_{K=02}$ states are studied. Also the roles of $B(E2, 0_2{}^+ - 2_g)$ and $B(E2, 0_2{}^+ - 2_\gamma)$ are discussed. Comparison with the dynamic pairing plus quadrupole model, for all the nuclei studied here, are made on a global basis. The lack of overlap in the wave function amplitudes $A_{200}(\beta, \gamma)$ of 0_2^+ and $A_{100}(\beta, \gamma)$ of the ground state also explains the reduced $B(E2, \beta - g)$ strength. The $B(E2, 2_\beta \to 0_\beta)$ is a good measure of the rotational collectivity (deformation) of the band. Shape coexistence at $N = 88, 90$ nuclei is reviewed. The possibility of $K^\pi = 0_2{}^+$ as a $\gamma\gamma$-vibration, when allowed by energy, in expected cases is examined. The interacting boson model predictions are also considered as required.

1 Introduction

The even-Z even-N nuclei in the medium mass region ($A = 140$–180), away from closed shells, develop collective level structure with increasing valence nucleons. The low-lying collective levels of positive (or negative) parity may be grouped into phonon multiplets or K-bands. The levels of each K-band may have a rotational or vibrational structure or an intermediate one. For positive-parity levels, usually one has a $K^\pi = 0_1{}^+$ yrast ground band, a $K^\pi = 2^+$ γ-band, and a $K^\pi = 0_2{}^+$ band. In the geometric view of the Bohr-Mottelson (BM) model, the $K^\pi = 2^+$ band is built on the axially asymmetric intrinsic vibration in the γ variable, and the $K^\pi = 0_2{}^+$ band is built on the axially symmetric intrinsic quadratic β-vibration [1]. In the $SU(3)$ limit of the algebraic Interacting Boson model-1 [2], the $K^\pi = 0_2{}^+, 2_1^+$ bands belong to the ($2N$-4, 2) irrep and are degenerate.

Empirically, while the ground band exhibits a systematic variation in level spacing with N and Z, the $K^\pi = 2^+$ γ-band head energy varies in a complex way. The characteristics of the $K^\pi = 0_2{}^+$ band are much more varied. A similar difference is in the interband $B(E2)$ ratios, in their deviation from the Alaga rules [1,3]. The linear band mixing perturbation approach breaks down much more, for the $K^\pi = 0_2{}^+$ β-band than for the $K^\pi = 2^+$ γ-band [3]. An interesting issue arose with the advent of the algebraic interacting Boson model (IBM) [2]. In the linear band mixing approach of BM model, the γ-β interaction was a second-order effect [1,3], while in IBM-1, the β-γ-interaction is predicted to be strong [2,4]. A nice review of the robust predictions of the IBM is given in ref. [4]. The stronger β-γ interaction and weaker β-g interaction led to a suggestion that the $K^\pi = 0_2{}^+$ band may be built on the 2γ vibration [5]. So that not all $K^\pi = 0_2{}^+$ bands are the bands representing the collective axially symmetric β-vibration. This aspect of $K^\pi = 0_2{}^+$ bands has been the subject of controversy and discussion in the last two decades [6–8].

Another anomaly concerns the notion of the shape coexistence *viz.* the proposition of a spherical $0_2{}^+$ state with a deformed ground state (*e.g.* in ^{152}Sm) [9], and a deformed $0_2{}^+$ state with a spherical ground state (*e.g.* in ^{150}Sm) [10]. This view was reinforced by the interpretation of the $0_2{}^+$ excitation cross section σ_{2n} data for $2n$ transfer in (p, t) and (t, p) reactions [11].

In most of the earlier works, the nature of the $0_2{}^+$ state was studied for individual nuclei. There is a need for a global review on a broad region of nuclei to have better appreciation of this problem. Hence, we present extensive data [12] which give the variation of $E(0_2{}^+)$ and $E(2_\gamma)$, to look for regularities. Garrett has noted [7] that the β-band in IBM or $SU(3)$ is different from the one in the geometric view [1]. In the present work, by the term β-band we shall mean the geometric view. In sect. 2, we survey the energy variation of $E(0_2{}^+)$ and $E(2_\gamma)$ with N, Z over the whole $A = 140$–180 (Ba-Hf) region and

[a] e-mail: jbgupta2011@gmail.com

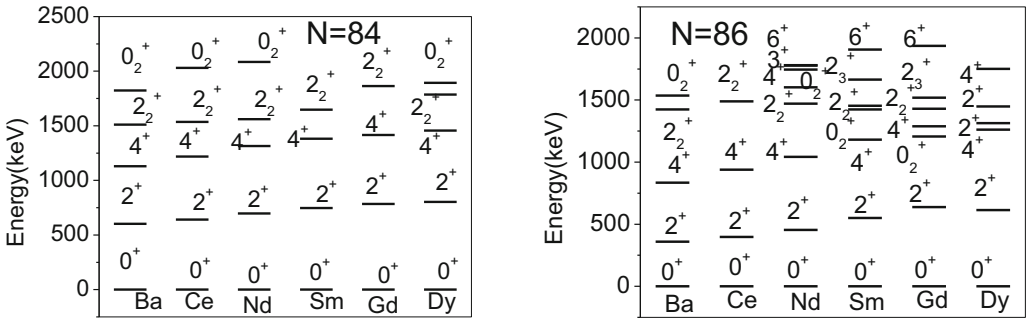

Fig. 1. Energy levels at $N = 84$ and $N = 86$ (Ba-Dy).

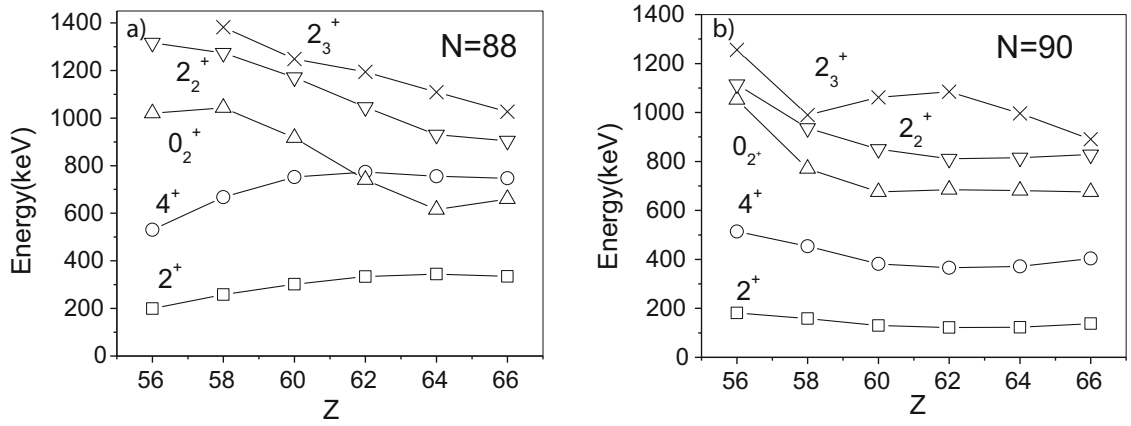

Fig. 2. Panel (a): $N = 88$ energy levels. The 2_2^+ are correlated with $0_2{}^+$, $2_3 = 2_\gamma$ lie higher. Panel (b): $N = 90$ energy levels. The $K^\pi = 0_2{}^+$ band are well visible. $2_3 = 2_\gamma$ lie above $2_2 = 2_\beta$.

illustrate the regularities. In sect. 3, we study intra band and inter band $E2$ transition rates and compare them with predictions of dynamic pairing plus quadrupole (DPPQ) model [13] from earlier works on a global scale and also for individual nuclei. Since the predictions of theory were not available for some nuclei, we did calculations for them. The discussion is given in sect. 4.

2 Low-energy level structure

2.1 Empirical survey

First we study the variation of the β-band head energy with N, Z to search for a regular pattern corresponding to a quadratic vibration in the β-degree of freedom.

2.1.1 $N = 84$–86 levels in Ba-Dy

At $N = 84$ with energy ratio $(E_4/E_2) = R_{4/2} < 2.0$, the two phonon triplets are well split and the $0_2{}^+$ state lies much above the 4_1^+ and 2_2^+ states (fig. 1). At $N = 86$, $R_{4/2} > 2.0$, and with increasing protons, the $0_2{}^+$ state tends to be a part of the two phonon triplet $(4_1, 2_2, 0_2)$ (fig. 1). The higher states are condensed into each other [12]. Using the pairing plus quadrupole interaction (PPQ) [13] for ^{148}Sm, the $V(\beta, \gamma = 0)$ potential well, which corresponds to an anharmonic vibrator, was obtained [14], *i.e.* the minimum lies at $\beta = 0$, but the shape is asymmetric in β variable. The state $I^\pi = 2_2^+$ has $> 50\%$ $K = 2$ component. In ^{150}Gd, the $0_2{}^+$ state moves below $I^\pi = 4_1^+$, 2_2^+. Thus, the K-band formation is developing with increasing Z. Also multiple $K^\pi = 0^+$ states are assigned [12], which may be two quasi-particle states. In the $U(5)$ symmetry [2], a triplet of states $(4_1{}^+, 2_2{}^+, 0_2{}^+)$ is expected.

2.1.2 $N = 88$–90 levels

At $N = 88$, the energy ratio $R_{4/2}$ exceeds 2.2 (2.65 to 2.2 for Ba-Dy) and the intrinsic excited vibrational bands lie separate from the ground band in Ba, Ce. In Nd-Dy, a triplet of $(0_2{}^+, 4_1{}^+, 2_2{}^+)$ seems to be forming (fig. 2(a)). But the state $2_2{}^+$ is not $K = 2$. Rather, it is $K^\pi = 0^+, 2_\beta$, forming part of a $K^\pi = 0_2{}^+$ band. The movement of 2_2^+ along with $0_2{}^+$ *versus* Z is a significant indicator of K-band formation (fig. 2(a)). Thus instead of a two-phonon triplet formation of $I^\pi = (4_g, 0_2{}^+, 2_\gamma)$, these levels appear as ground band, $K^\pi = 0_2{}^+$ β-band and $K^\pi = 2^+$ γ-band.

The same pattern continues at $N = 90$, with the distinction that now the energy ratio $R_{4/2}$ is about 2.90 for Nd, Sm, Gd, Dy (fig. 2(b)). This ratio is a first signature of the critical point symmetry $X(5)$ [15], serving as the bench mark of the turning point from the shape transitional (β-soft) to a rotor regime. In $X(5)$ symmetry which has an analytic solution under approximate separation of β, γ

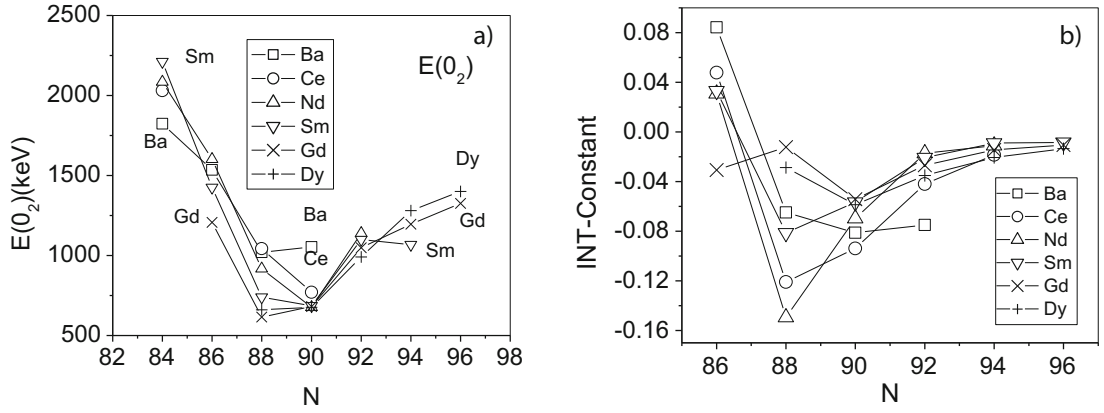

Fig. 3. Panel (a): $E(0_2)$ *versus* N for Ba-Dy, a valley is formed at $N = 88$–90. Panel (b): Rot.-vib. interaction coefficient c *versus* N for Ba-Dy. The valley at $N = 88$–90 corresponds to that of $E(0_2)$.

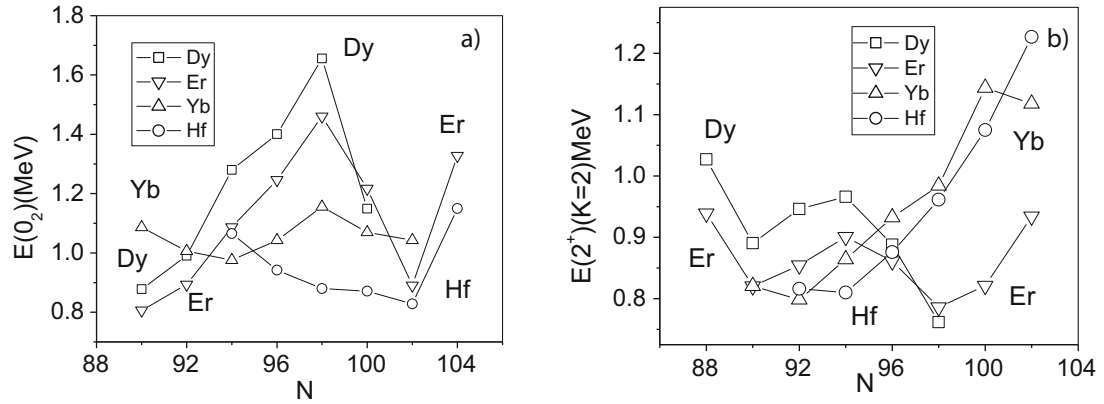

Fig. 4. Panel (a): The variation of $E(0_2)$ *versus* N for $Z = 66$–72. A peak is formed at $N = 98$. Panel (b): Variation of $E(2_\gamma)$ *versus* N for Dy-Hf. A peak is formed at $N = 94$, and a valley at $N = 98$.

degrees of freedom, one gets $R_{02} = E(0_2{}^+)/E(2_1^+) = 5.65$, which almost agrees with $N = 90$ nuclei (= 5.20, 5.58, 5.53, 4.90) Nd, Sm, Gd, Dy, respectively. The $K^\pi = 0_2{}^+$ state lies below the $K^\pi = 2^+$ γ-band head (fig. 2(b)). The nucleus needs less energy to execute axially symmetric vibration than γ-asymmetric vibration. In fact this defines their β-soft character.

2.1.3 A valley at $N = 88$–90

The variation of $E(0_2{}^+)$ with N for Ba-Ce-Dy is illustrated in fig. 3(a). A valley is formed at $N = 88$–90. The Ba, Ce $E(0_2{}^+)$ data at $N = 88$ lie higher and Ba lies higher at $N = 90$. The three proton pairs in Ba provide less deformation effect. It is remarkable that the $E(0_2{}^+)$ value is almost constant at $N = 90$ for Nd-Dy. A microscopic explanation of the constancy of nuclear structure at $N = 90$ in Sm-Dy was given in terms of the filling of nucleons in Nilsson orbits in ref. [16]. It was shown that the down sloping neutron orbitals beyond $N = 82$ control the deformation of the nuclear core. At the same time, the proton orbitals beyond $Z = 60$ fill two almost horizontal orbitals, so that the protons filling at $Z = 60$–66 have little effect on the deformation. Clark *et al.* [17] made a detailed band mixing analysis of ^{150}Nd and ^{152}Sm. They interpreted the $K^\pi = 0_2{}^+$ state as a β-vibration.

In the rotation-vibration interaction (RVI) model, the ground band level energy is given by

$$E(I) = aI + bI(I+1) + cI^2(I+1). \qquad (1)$$

For the shape transitional nuclei, the RV interaction constant "c" is a measure of the rotation vibration mixing. A plot of "c" for this region (fig. 3(b)), exhibits a valley at $N = 88$–90, which has a similarity with the valley for $E(0_2{}^+)$ in fig. 3(a). At $N = 90$, $|c|$ is large, which corresponds to low $0_2{}^+$. The spread in c at $N = 88$, corresponds to the spread of $E(0_2{}^+)$. The rise of c (decrease towards zero) at $N = 86$ and $N = 92$–96, correspond to the rise of $E(0_2{}^+)$.

2.1.4 Other nuclei ($Z \geq 66$)

For $Z = 66$–72, Dy-Hf, the variation of $E(0_2{}^+)$ with N is illustrated in fig. 4(a). While the energy ratio $R_{4/2}$ increases with increasing N ($N < 104$), the $K^\pi = 0_2{}^+$ state lies above 2_γ, except in ^{158}Er, ($N = 98$ Hf and $N = 100$, 102 Yb, Hf) [12]. In these nuclei, the $0_2{}^+$ state rises up

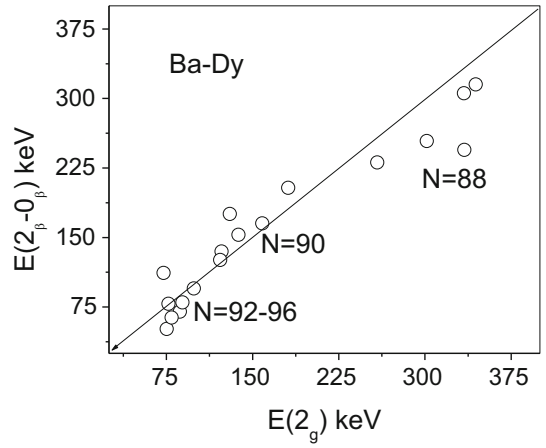

Fig. 5. The energy difference $E(2_\beta - 0_\beta)$ *versus* $E(2_g)$ for Ba-Dy ($N = 88$–96). Continuous line is the diagonal.

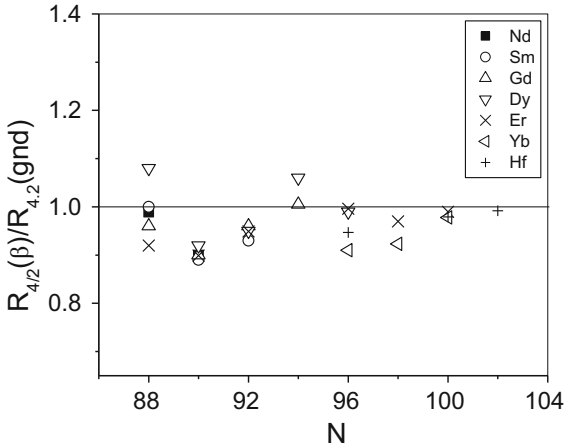

Fig. 6. Ratio of $R_{4/2}$ in β-band relative to ground band *versus* N for Nd-Hf.

with neutron number N and a peak is formed at $N = 98$ for Dy, Er, Yb. On the other hand, $E(2_\gamma)$ forms a smaller peak at $N = 94$ and a valley at $N = 98$ for Dy, Er (fig. 4(b)). Consequently, $K^\pi = 0_2{}^+$ band lies above 2_γ at around $N = 98$ (except in Hf). Contrary to a general impression, the band heads of $K^\pi = 0_2{}^+$ and $K^\pi = 2^+$, both exhibit a coupled varied dependence on N, Z, but with maxima at different N. At $N = 88$–90 both bands go down. The rise and fall of $0_2{}^+$ and 2_γ at certain neutron numbers reflects the role of the Nilsson single particle orbits near the Fermi surface, and the filling of neutrons and protons in these orbitals [1].

2.1.5 $K^\pi = 0_2{}^+$ band spread in Ba-Dy ($N < 104$)

Note that the energy difference $E(2_\beta - 0_\beta)$ in β-band is almost the same as $E(2_g - 0_g)$ in the ground band for Ba-Dy nuclei for all N (see fig. 5). The $N = 88$ data lie slightly below the diagonal, and the $N = 90$ data lie slightly above the diagonal. Similarly the $N > 90$ data are close to the diagonal but below it. Thus the rotational bands built on $K^\pi = 0_2{}^+$ state and ground state have almost the same moment of inertia. This fact supports the similar deformation of $K^\pi = 0_2{}^+$ bands. Using the square potential of infinite depth in the $X(5)$ symmetry analytic solution of $H_{\rm BM}$, one gets slightly expanded β-band level spacing [15]. In the confined beta soft (CBS) model with adjustable square potential width and location, agreement with experiment can be achieved [18]. As seen in fig. 6, the ratios of $R_{4/2}$ in β-band and ground bands *versus* N for Nd-Hf deviate from 1.0 by 10% or less.

2.1.6 Correspondence with VMI stretching constant C and the CBS model

Chou *et al.* [8] observed a correlation of $E(0_2{}^+)/E(2_1^+) = R_{02}$ with the energy ratio $R_{4/2}$. The rise of the β-band head in this region of axially symmetric deformed nuclei ($N > 90$) is exhibited in a plot of the ratio R_{02} *versus* $R_{4/2}$ (fig. 7(a)). The ratio R_{02} rises slowly at low $R_{4/2}$. The four lowest points (of Gd, Dy, Er and Sm) correspond to the $N = 88$ valley in fig. 3. The four $N = 90$ isotones (Nd-Dy) lie at $R_{4/2} = 2.90$. Beyond $X(5)$, the beta band head rises fast. The high point of ^{164}Dy corresponds to the peak at $N = 98$ in fig. 4(a).

Using the confined beta soft (CBS) model, Pietralla *et al.* [18] linked this variation to the variation of $r = \beta_m/\beta_M$, the ratio of β *versus* the full width β_M of the square well potential, which defines the stiffness of the square well. The complex variation of $E(0_2{}^+)$ apparent in fig. 4(a), is smoothened in the plot of R_{02} (fig. 7). The CBS model fit accounts for the varying deformation of the nuclear core and its stiffness, which is strongly affected by the ratio $r = \beta_m/\beta_M$,

$$\text{Eigenvalues in CBS } E_{L,s} = (\text{const}/\beta_M^2)(z_{L,s}{}')^2. \quad (2)$$

The $z_{L,s}{}'$ represent the s-th zero of the Bessel solutions. The scale parameter β_M was adjusted and the calculation reproduces this variation approximately [18].

The rigidity of the nuclear core can be expressed in terms of the stretching constant "C" in the potential term of the variable moment of inertia formula [19]:

$$E(I) == \hbar^2 I(I+1)/2\theta_I + (1/2)C(\theta_I - \theta_0)^2. \quad (3)$$

Using an $\theta_I = \theta_0(1 + \sigma I)$ approximation, we have solved the VMI equation and estimated the stretching constant C for Nd-Hf nuclei in the $N < 104$ region. The plot of C *versus* energy ratio $R_{4/2}$ in fig. 7(b) illustrates the soft core below the $X(5)$ symmetry point, and the transition to the rigid core represented by the rapidly increasing value of C between $X(5)$ and the rotor limit. The similar variation of C and R_{02} illustrates their correlation as also illustrated in the CBS solution. There is good (nearly one to one) correspondence of the R_{02} data and the C data (figs. 7(a) and (b)).

For a further study of the $K^\pi = 0_2{}^+$ band structure, we have used the Soft Rotor Formula (SRF) [20],

$$E_I - E_{02} = \text{const } I(I+1)/\theta_0(1 + \sigma I), \quad (4)$$

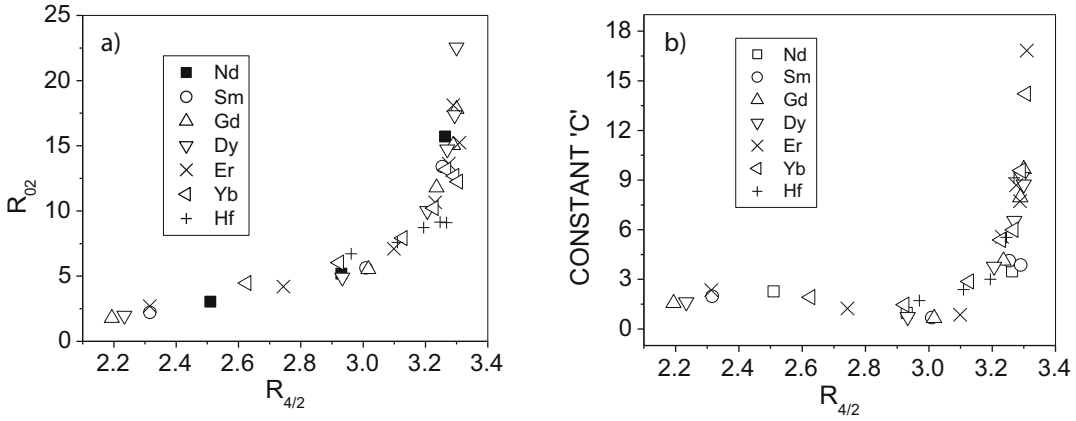

Fig. 7. Panel (a): The energy ratio $R_{02} = E(0_2)/E2_1$ *versus* $R_{4/2}$. for Nd-Hf. Panel (b): The VMI stretching constant C *versus* $R_{4/2}$.There is a nearly one to one correspondence between C and R_{02}.

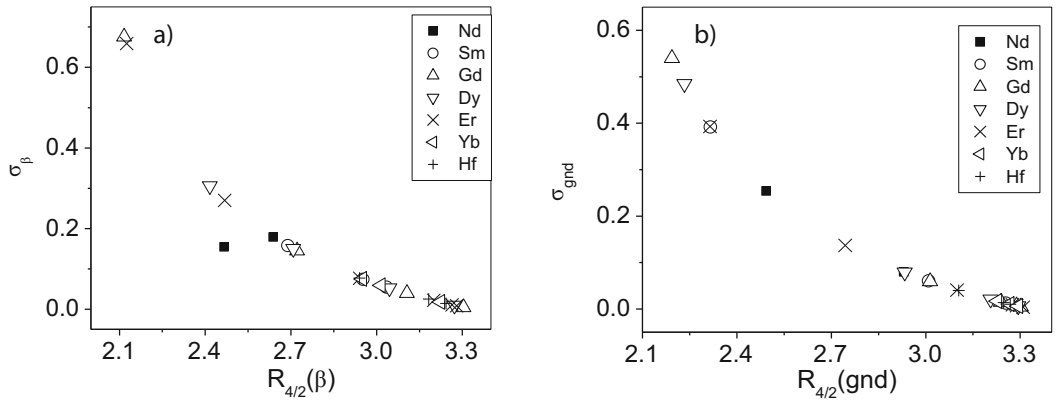

Fig. 8. Panel (a): Softness parameter σ (SRF) β-band *versus* $R_{4/2}$ (β). Panel (b): Softness parameter σ (SRF) of ground band *versus* $R_{4/2}$ (gnd).

to evaluate the softness parameter $\sigma(\beta)$ for the $K^\pi = 0_2{}^+$ bands for the nuclei considered here. A comparison of $\sigma(\beta)$ *versus* $R_{4/2}(\beta)$ with $\sigma(g)$ *versus* $R_{4/2}(g)$ for ground bands illustrates their good correspondence (figs. 8(a) and (b)).

2.1.7 Role of energy level systematics on the nature of $0_2{}^+$ states

The energy systematics of $0_2{}^+$ and 2_γ play an important role to understand the nature of $K^\pi = 0^+, 2^+$ bands. The role of quadrupole deformation in terms of a vibrating-rotating nuclear core is evident. The shifting peaks reflect the essential role of Nilsson orbits near the Fermi surface. The operator r^2Y_{20} generates the collective $K^\pi = 0^+$ vibration, and $r^2Y_{2\pm2}$ the $K^\pi = 2^+$ γ-vibration [1,7]. Nilsson wave functions having $\Delta\Omega = \Delta\Lambda = 0$ and $\Delta N = \Delta n_z = 2$ couple non-diagonal matrix elements of r^2Y_{20}. For $r^2Y_{2\pm2}$, $\Delta\Omega = \Delta\Lambda = 2$ and $\Delta N = 0$, 2, $\Delta n_z = 2$ combinations couple. The availability of such couplings at different N, Z leads to rise and fall of $0_2{}^+$ and 2_γ (and weak β-g strength) and to the triaxiality and γ-softness. The $r^2Y_{2\pm2}$, couplings are available at $N = 98$, in Dy when the subshell is half-filled (see [1], p. 552). However, the behavior of the weakly collective $0_2{}^+$ state with N and Z is more erratic and its understanding involves other degrees of freedom as well.

A comparison of level energies of $0_2{}^+$ *versus* 2_γ shows that in 16 lighter nuclei (Ba-Hf) (figs. 2–4), 0_2 lies below 2_γ. They represent one quadrupole phonon vibration [1]. In other neutron-rich nuclei, out of 22 cases cited here, in 4 cases again, $0_2{}^+$ lie below 2_γ. In another 4 cases, $0_2{}^+$ lie above 2_γ, but within 50–70 keV. So no two $\gamma\gamma$ phonon probability arises. In the other cases (^{160}Gd, $^{160\text{-}164}$Dy, $^{162\text{-}168}$Er, $^{160\text{-}166}$Yb, ^{166,168}Hf), $0_2{}^+$ lies above 2_γ. A preliminary view is that in a well-deformed nucleus, the core is hard, with narrow $V(\beta, \gamma = 0)$ or equivalently narrow square well potential [18]. So the decay probability to the g-band is expected to be small. Also, see sect. 3.3 for the role of wave functions. At higher energy, a 2γ phonon view is possible [21,22]. Also pairing vibrations can compete [7].

Meyer *et al.* [23] did an extensive survey of $K^\pi = 0^+$ states in the rare-earth region. They have listed the 0^+ states lying below twice $E(0_2{}^+)$ and above it. In several nuclei more than one 0^+ states were seen. So they compared them with pairing vibration energy excitation data and found them below it.

3 B(E2) values

3.1 The DPPQ model

The dynamic pairing plus quadrupole (DPPQ) model of Kumar-Baranger [13] is well suited to provide some evidence on the nature of $K^\pi = 0_2{}^+$ bands and for the predictions of the absolute $B(E2)$ values. The model is microscopic in the sense that the parameters of the $H_{\rm coll}$ are obtained from the solutions of $H_{\rm PPQ}$.

$$H_{\rm coll} = V(\beta,\gamma) + T_{\rm vib}(\beta,\gamma) + T_{\rm rot}(\beta,\gamma), \quad (5)$$

$$H_{\rm coll}\Psi_{\alpha IM} = E_I\Psi_{\alpha IM}, \quad (6)$$

$$\Psi_{\alpha IM} = \Sigma_{(K={\rm even},+ve)}A_{\alpha IK}(\beta,\gamma)\phi^I_{MK}. \quad (7)$$

ϕ^I_{MK} are the symmetrized sums of the rotational D functions, $A_{\alpha IK}(\beta,\gamma)$ are the intrinsic vibrational wave function amplitudes. Coefficient α are counting index for the states of same spin I.

The $H_{\rm PPQ}$ is built on spherical single-particle basis, to which quadrupoole and pairing interactions are added on equal footing in the generalized Bogolyubov transformation (GBT) method,

$$H_{\rm PPQ} = H_S + H_Q + H_P. \quad (8)$$

The solution of the $H_{\rm PPQ}$ yields quasi-particle energies and q.p. wave functions. This is done for a mesh of 92 points in the (β,γ) space (β = 0–0.5; $\gamma = 0°$–$60°$). Using standard relations, the parameters of the collective Bohr Hamiltonian $H_{\rm coll}$ are derived for all the mesh points of the (β,γ) space. Then a summation of the collective wave functions over the full (β,γ) space provides the dynamics of the motion of the nuclear core. Thus a full band mixing is achieved (see [14,24–26] and references cited therein). Slight variation of the quadrupole force strength $\chi = X_Q \times A^{-1.4}$ (MeV) is allowed to approximately reproduce the energy scale in $E(2^+_1)$. Also the ($Z = 40$, $N = 70$) inert core effect is taken into account through the mass renormalization factor F_B, which multiplies all the inertial coefficients in $T_{\rm vib}$ and $T_{\rm rot}$ (eq. (5)).

Kumar and Gupta [24] reproduced the relative positions of 2_β, 2_γ in $^{152\text{-}160}$Gd. The spectra of $^{146\text{-}152}$Sm, ^{154,156}Dy and ^{158,160}Dy were studied in refs. [14,25,26], respectively. Though the vibrational energy scale is somewhat enhanced, the over all spectral features and the $E2$ transition rates were well reproduced. Here we have extended the DPPQ model calculation to ^{162,164}Dy and the $^{162\text{-}168}$Er isotopes as well (tables 1 and 2).

3.2 Absolute B(E2) values

Besides the energy spectra, one has to consider the absolute $E2$ decay strength as a measure of the collectivity of the nuclear states. In tables 1 and 2 we have listed the relevant $B(E2)$ values for some nuclei (Nd-Er, $N < 104$) and compared with the predictions from DPPQ model.

The absolute $B(E2, 0_g \rightarrow 2_g)$ values are available from Coulomb excitation and life time data for most nuclei [12, 27]. A plot of these values for the Nd-Dy region is given in fig. 9 (see tables 1, 2). As is well known, $B(E2, 0_g \rightarrow 2_g)$ increases with N (increasing valence neutrons), *i.e.* increasing deformation and saturates at large N. These values are also used for fixing the strength of the quadrupole force in DPPQ model and the charge in the quadrupole operator in IBM and for normalization of other $B(E2)s$. The charge parameter $e_n = 0.6$ (or 0.7) ($e_p = 1 + e_n$) was kept constant in the DPPQM calculations. Most values are in close agreement with experiment (table 1).

For studying the collectivity of $K^\pi = 0_2{}^+$ band, $B(E2, 2_{02} \rightarrow 0_2)$ are compared with $B(E2, 2_g \rightarrow 0_g)$ (= 1/5 of $B(E2, 0_g - 2_g)$, listed in table 1). However, not much data are available for the former. The DPPQ model [13] is well suited for studying the variation of absolute $B(E2)$ values. Hence we compare the experimental data with the values from the DPPQ model in the microscopic approach (see table 1). The plot of DPPQM $B(E2, 2_{02} \rightarrow 0_2{}^+)$ *versus* $B(E2, 2_g \rightarrow 0_g)$ exhibits a close relationship between the two (fig. 10). Most data points lie on or near the diagonal within 10%. This supports the collective rotational bands built on the $0_2{}^+$ state. This fact is known but has not been given the emphasis it deserves.

The inter-band $E2$ decay strength for $K = 2$, γ-g transitions are much weaker, as expected. The $B(E2, 0_g - 2_\gamma)$ in Nd-Er region lie around 0.12 $e^2b^2 \cdot (\sim 25$ W.u.) in experiment, with a few exceptions (at $N = 90$, Gd, Dy) (fig. 11(a)). Also the values fall with increasing N (deformation), and rise with increasing Z for a given N. The DPPQM values from our calculation (tables 1, 2 and fig. 11(b)) also exhibit a pattern similar in magnitude and form, though there are deviations in particular cases. The average is again 0.12 e^2b^2.

Next we look at $B(E2, 0_g \rightarrow 2_\beta)$ values *versus* N (tables 1, 2, fig. 12). These are $\sim 1/6$ of $B(E2, 0_g \rightarrow 2_\gamma)$, (see last column of table 1). The data form two sets corresponding to quadrants one ($Z < 66$, but including $N = 90$ Dy) and quadrant two ($Z \geq 66$). In each set, the value falls with increasing N. The average value is ~ 0.02 e^2b^2. Again, the DPPQM values reproduce a similar overall pattern (fig. 12)) including the low $N = 90$ Dy value and the relatively higher values for Dy, Er isotopes in quadrant 2 ($N \geq 94$). It is well known [4,28] that $B(E2, 0_g - 2_\beta)$ are less than $B(E2, 0_g - 2_\gamma)$. In IBM it is predicted naturally [4]. In DPPQ model, involving profound band mixing, also this was generally predicted [14,25,26], as illustrated here.

Next look at $\beta \rightarrow g$ transitions: $B(E2, 0_2{}^+ - 2_g)$ *versus* N (table 1, 2 and fig. 13). Only few data are available. But a definite pattern emerges. The values fall with increasing N. The same pattern is reproduced in DPPQM (more data points) (fig. 13). The β-softness at $N = 88$–90 as exhibited in fig. 5 for $E(0_2)$, is also reflected in the values of $B(E2, 0_2{}^+ - 2_g)$ here in experiment and theory. Also, the lowest values at $N = 96$–100 (Gd, Dy, Er) of about 5 W.u. are systematically predicted in the calculation based on $H_{\rm coll}$, which implies a coherent motion of the nucleons.

Table 1. Absolute $B(E2)$ values (e^2b^2) in experiment (first row) and theory (second row). $R = B(E2, 0_g - 2_\beta)/B(E2, 0_g - 2_\gamma)$. Experimental data are as in theory references, and [27].

Transition	$0_g - 2_g$	$0_g - 2_\gamma$	$0_g - 2_\beta$	$0_\beta - 2_g$	$2_\beta - 0_\beta$	$2_\gamma - 0_\beta$	R
^{148}Nd	1.42 5	0.084	0.024 5	0.20 8			0.29
DPPQ	1.72	0.064	0.033	0.39	0.27	0.084	0.52
^{150}Nd	2.72 4	0.09 1	0.013 1	0.21 4	0.45 15		0.14
DPPQ	2.73	0.115	0.004	0.204	0.49	0.007	0.036
^{150}Sm	1.32 7	0.115 4	0.015 5	0.26 3	0.44 26	0.124 60	0.14
DPPQ	1..72	0.062	0.035	0.40	0.28	0.082	0.57
^{152}Sm	3.37 5	0.090 12	0.023 2	0.16 4			0.26
DPPQ	3.16	0.112	0.0115	0.165	0.65	5 E−04	0.103
^{154}Sm	4.36 5	0.080 13	< 0.023	0.06			0.29
DPPQ	3.84	0.112	0.028	0.094	0.88	1.2 E−05	0.25
^{152}Gd	1.58 15		0.007 1	0.85 20			
DPPQ	1.63	0.057	0.046	0.71	0.275	0.039	0.81
^{154}Gd	3.85 8	0.14 1	0.021 4	0.21 3	0.60 5		0.15
DPPQ	3.86	0.139	0.019	0.22	0.76	7 E−04	0.14
^{156}Gd	4.57 5	0.120 4	0.016 4	0.150			0.133
DPPQ	4.35	0.143	0.020	0.115	0.82	0.009	0.14
^{158}Gd	4.97 5	0.085 5	0.008 1	0.006			0.094
DPPQ	4.60	0.098	0.070	0.084	0.74	0.038	0.71
^{160}Gd	5.15 6	0.101 3					
DPPQ	5.18	0.111	0.052	0.051	0.94	0.0096	0.47
^{154}Dy	2.39 12						
DPPQ	2.27	0.066	0.069	0.56	0.30	0.16	1.04
^{156}Dy	3.72 3	0.180 11	0.008				0.044
DPPQ	3.83	0.168	0.002	0.26	0.66	0.015	0.012
^{158}Dy	4.67 4	0.149 8	0.053 8				0.36
DPPQ	4.82	0.167	0.022	0.118	0.94	0.004	0.13
^{160}Dy	5.06 13	0.116 8	0.016 2				0.155
DPPQ	4.77	0.111	0.073	0.094	0.73	0.046	0.66

Factors of 20 variations are reproduced here (see tables 1 and 2 and fig. 13).

3.3 Role of state wave functions

In figs. 14 and 15 we illustrate the wave functions of the ground state, $I^\pi = 0_2{}^+$ state and $KI = 22$ state, respectively, of ^{156}Gd, on the (β, γ) space, obtained in DPPQ model calculation in ref. [29]. The wave function spreads of other states in the same band are similar. From these plots, it is apparent, that the overlap of the β-wave function (which has a node in the middle) with the ground state wave function is the least, which explains the smallness of $B(E2, 0_g - 2_\beta)$ compared to $B(E2, 0_g - 2_\gamma)$. The dynamics of the DPPQM cited above (sect. 3.1) takes into account the summation over the full (β, γ) space.

In the exact numerical solution of the BM collective Hamiltonian at or near the $X(5)$ symmetry based on an algebraic collective model (ACM), Caprio *et al.* [30] studied the probability distribution of the wave functions of ground, β-band and γ-band for three assumed values (a = 0, 200, 1000) of the γ-stiffness parameters $a = 2AB\beta_w^2/\hbar^2$ (B = mass parameter, $V(\gamma) = A\gamma^2$) (fig. 16). These probability distributions are similar to those of the ones exhibited in figs. 14 and 15. This is an important point, when considering the nature of a $0_2{}^+$ state, *vis à vis* the β-g decay strength in the earlier studies [6–8].

3.4 Individual nuclei

As stated in sect. 1, the strong γ-β transition predicted in IBM is different from the linear 3-band mixing theory (valid only for small deviations from the rotor model

Table 2. Absolute $B(E2)$ values (e^2b^2) in experiment [27,12] (first row), theory (second row), in Dy-Er. P = present calculation in DPPQ model.

Transition	$0_g - 2_g$	$0_g - 2_\gamma$	$0_g - 2_\beta$	$0_\beta - 2_g$	$2_\beta - 0_\beta$	$0_\beta - 2_\gamma$	Ref.
^{162}Dy	5.35 10	0.118 6					
DPPQ	5.98	0.110	0.061	0.082	1.19	0.16	[42], P
^{164}Dy	5.60 5	0.114 6					
DPPQ	6.57	0.119	0.031	0.035	1.37	0.028	P
^{160}Er	4.15 15						[12]
DPPQ[(a)]	4.566	0.209	0.0035	0.176	0.66	0.755	P
^{162}Er	5.01 5	0.104 8	0..042 7				[12]
DPPQ	5.16	0.117	0.093	0.092	0.85	0.046	P
^{164}Er	5.20 4	0.18 5	0.006 3				[12]
DPPQ	4.82	0.116	0.047	0.059	0.98	0.062	P
DDM	5.18	0.203	0.001			0145	[22]
^{166}Er	5.77 5	0.140 4	0.018 2	0.014 5		0.012 3	[46]
DPPQ	5.30	0.106	0.038	0.028	1.00	0.040	P
DDM	5.59	0.171	0.019			0.25	[22]
^{168}Er	5.77 6	0.131 8	< 0.02	0.002		0.017	[6]
DPPQ	5.80	0.159	0.043	0.073	1.14	0.032	[47]
DDM	5.73	0.141	0.032			0.29	[22]

[(a)] The corresponding $B(E2)$ values in IBM-1 are 4.26, 0.109, 0.007, 0.009, 0.63 and 0.050 e^2b^2 (see text).

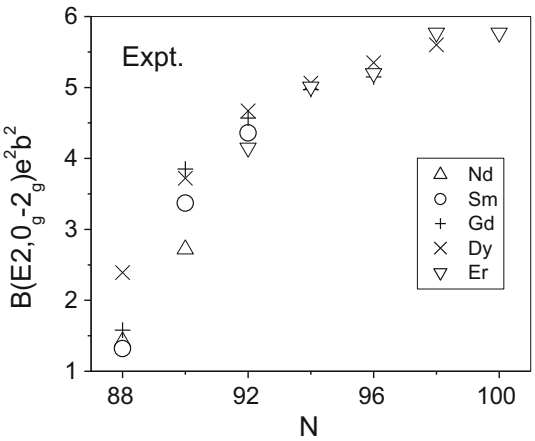

Fig. 9. Absolute $B(E2, 0_g \rightarrow 2_g)$ (e^2b^2) *versus* N in Nd-Er [27]. Initial fast rise and saturation for increasing N is exhibited.

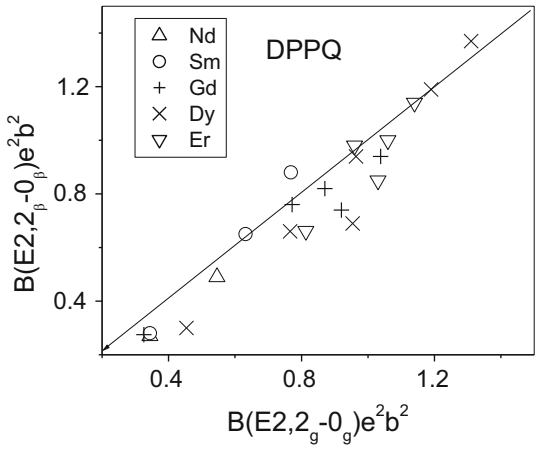

Fig. 10. Absolute $B(E2, 2_\beta \rightarrow 0_\beta)$ *versus* $B(E2, 2_g \rightarrow 0_g)$ from DPPQ model. Most data points lie on or near the diagonal, indicating similar deformation of the two bands.

and Alaga rules [31]). The prediction of $B(E2, 0_\beta - 2_\gamma) \sim B(E2, 0_g - 2_\gamma)$ in IBM was a new development [4,28]. In cases where the 2_γ state is close to $0_2{}^+$, the $E2$ transition $0_2{}^+ \leftrightarrow 2_\gamma$ is hard to observe. Only in those nuclei, in which 0_β lies high, a β-γ $E2$ transition may be measured. This led to the new experimental efforts, which we discuss for individual nuclei below. We also study the shape coexistence in a nucleus.

In ^{152}Sm, the large $B(E2, 0_2 \rightarrow 2_g) = 32$ W.u. ($0.16\, e^2b^2$) (table 1) supports a collective vibrational character of

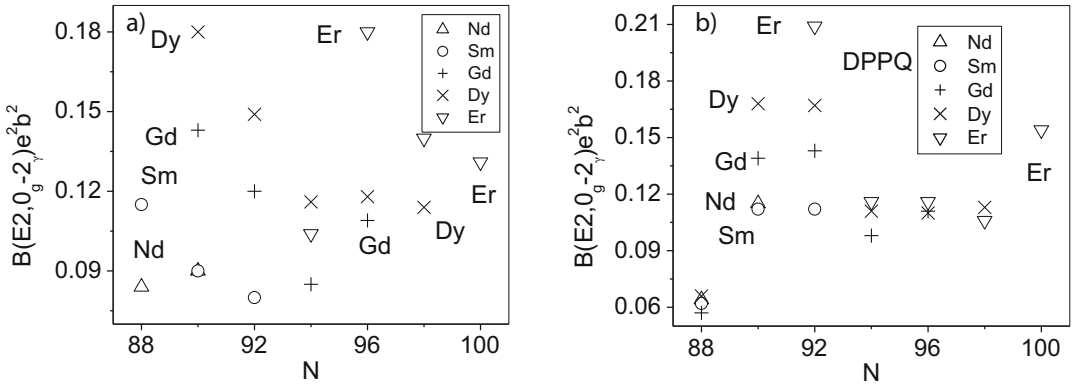

Fig. 11. Panel (a): $B(E2, 0_g - 2_\gamma)$ *versus* N for Nd-Er in experiment. The values fall for increasing N (deformation), and rise for increasing Z. Panel (b): $B(E2, 0_g \rightarrow 2_\gamma)$ *versus* N for Nd-Er from the DPPQ model.

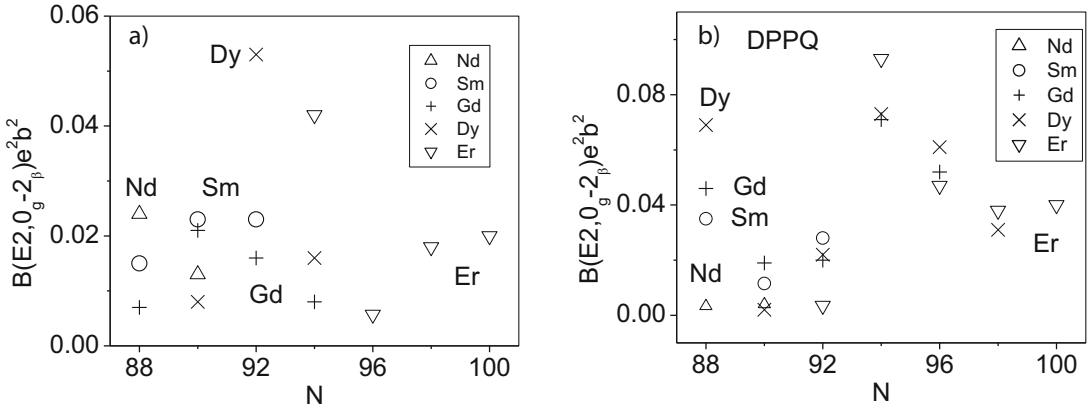

Fig. 12. Panel (a): $B(E2, 0_g - 2_\beta)$ *versus* N for Nd-Er in experiment. The data form two sets, corresponding to quadrant one ($Z \leq 66$) and two ($Z > 66$). In each set, the value falls with increasing N. Panel (b): DPPQ model values exhibit same trend, as in experiment.

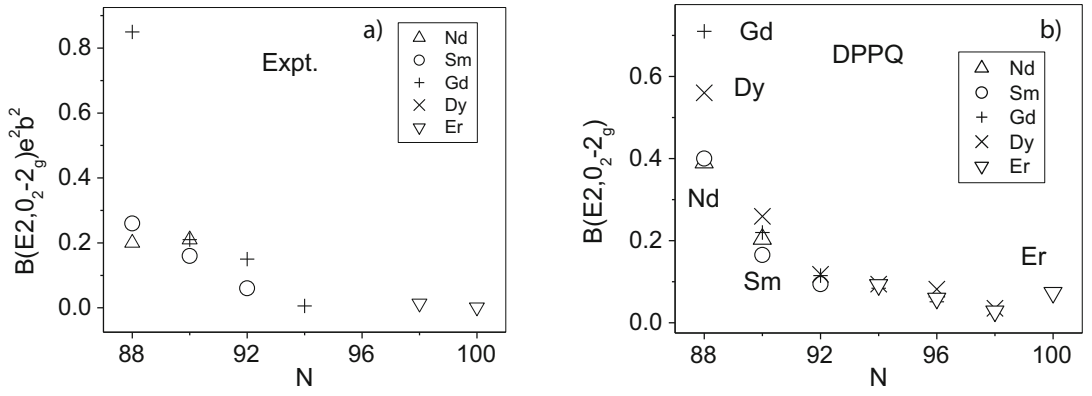

Fig. 13. Panel (a): $B(E2, 0_\beta \rightarrow 2_g)$ *versus* N in experiment in Nd-Er. The values fall with increasing N (deformation). Panel (b): $B(E2, 0_\beta - 2_g)$ *versus* N in Nd-Er from the DPPQ model exhibit same trend, as in experiment.

the $0_2{}^+$ state [7]. Through band mixing theory, Clark *et al.* [17] explained the data on β-g transitions in ^{152}Sm by band mixing calculation, as cited above. By comparison with microscopic theory results [32] in DPPQ model [13], they supported the β-vibration view. The same applies to other $N = 90$ isotones. In the alternative models (IBM and $X(5)$ critical point symmetry) with fewer free parameters alternative interpretations have also been given on the nature of $0_2{}^+$ state.

In ^{150}Sm, $B\,(E2, 0_2{}^+ \rightarrow 2_g)$ is even greater ($= 0.26$ e^{2}b^2), and is again reproduced in DPPQM [33] signifying a β-vibration. In ^{152}Gd, $B\,(E2, 0_2 - 2_g) = 0.85\,(20)$ e^{2}b^2 (~ 180 W.u.) signifies large $E2$ strength, which was also found in the microscopic DPPQ model calculation [34]. In

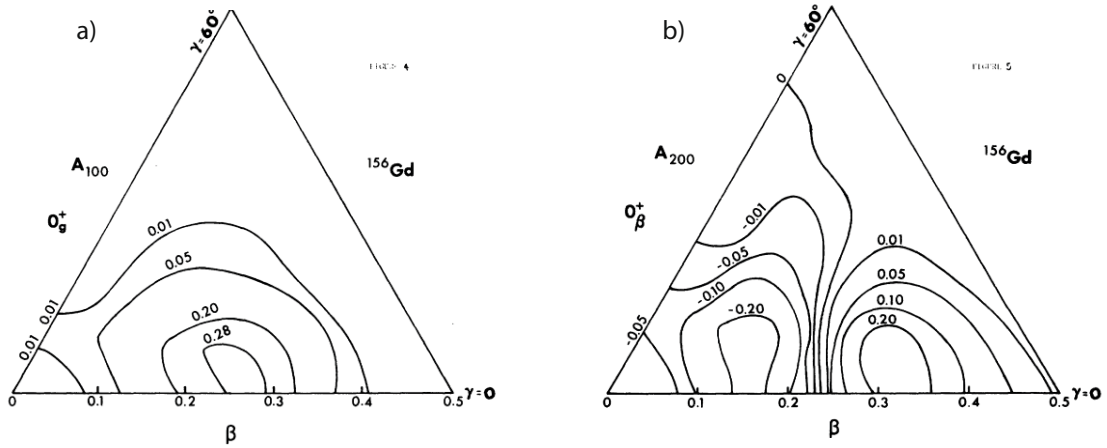

Fig. 14. Panel (a): Contour plots of the ground state wave function $A_{\alpha IK} = A_{100}$ of ^{156}Gd in (β, γ) space from DPPQ model [29]. Numbers on the wave function $A_{\alpha IK}$ amplitudes of eq. (6). (all signs are reduced to positive). Panel (b): Beta band (0_β) wave function A_{200} of ^{156}Gd from the DPPQ model [29]. A node is formed at the middle for the $n_\beta = 1$ wave function.

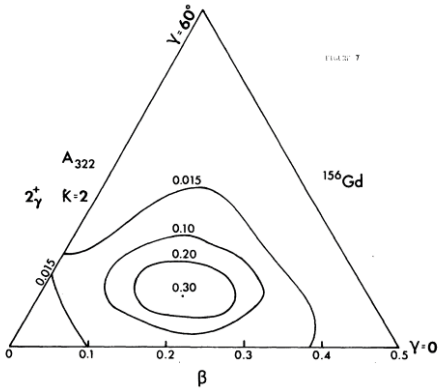

Fig. 15. The $K = 2$ component $A_{\alpha IK} = A_{322}$ of the 2_γ wave function of ^{156}Gd from DPPQ model [29]. The maximum amplitude 0.30 lies towards $\gamma = 30°$. The $K = 0$ component, not shown here, contributes 14% to the normalization of the wave function.

^{154}Dy, $B(E2, 0_2{}^+ \to 2_g) = 0.56$ e^{2}b^2, predicted in DPPQ model calculation [25], indicates good rotational collectivity.

3.4.1 Shape phase coexistence and shape transition in $N = 88$, $N = 90$

At $N = 88$–90, a shape phase transition occurs in Sm and Gd. Here, an interesting proposition of shape coexistence was made in the seventies [11]. Deformed excited $0_2{}^+$ excited states in $N = 88$ Sm, Gd, and excited spherical $0_2{}^+$ states in deformed ground state nuclei at $N = 90$ were suggested. In the shape coexistence view, the finite 2n transfer cross section was explained assuming a deformed $0_2{}^+$ state in ^{150}Sm. In a detailed study of $B(E2)$ values and interband transition rates in IBM-1 and DPPQ model in ref. [33], a similarity of β-band to ground band was illustrated. Also the $0_3{}^+$ state in ^{150}Sm has a 2β character, with strong decay to the $K^\pi = 0_2{}^+$ band, and with the same deformation [33]. Thus the shape coexistence view in ^{150}Sm does not appear to be supported by data.

Regarding the spherical character of the $0_2{}^+$ state in ^{152}Sm, Kumar [32] explained the large (p, t) cross section for 2n transfer for the excited state [11]. According to recent findings [35], it is explained that a large 2n cross section of an excited 0_2 state [11] arises due to shape difference between the target and product nucleus. According to DPPQ model calculations, almost the same deformation is obtained for the three K-bands in ^{152}Sm and ^{154}Gd [36].

3.4.2 Deformed nuclei $N > 90$

At $N = 92$, in ^{152}Nd, the $0_2{}^+$ state rises to 1139 keV, with a 2_2^+ state at 1251 keV. $2_2 = 2_\beta$ decays to 0_g, 2_g, 4_g. The $B(E2, 2_\beta - 2_1/4_1) = 0.35(4)$ is reproduced in the DPPQ model [37]. The $B(E2, 2_2 - 0/2) = 0.21(4)$ agrees with DPPQ model value of 0.215.

^{154}Sm with $R_{4/2} = 3.2$ is a well-deformed nucleus. Krucken *et al.* [38] measured life times by Coulomb excitation. Two excited $0_2{}^+$, $0_3{}^+$ states, at 1100 keV and 1203 keV, were identified. Here $B(E2, 0_2{}^+ - 2_1{}^+) =$ 12 W.u. = (0.06 e^{2}b^2) favors it as a good example of a beta vibration [38]. The second excited $K^\pi = 0_3{}^+$ excitation, below 2_γ state is relatively (40 times) weaker and a very weak band mixing is indicated. The $2_4 = 2_\gamma$ lies higher, with $B(E2, 2_\gamma - 0_1/2_1) = 0.69$ equal to the Alaga value, while the $B(E2, 2_\beta - 0_1/2_1) = 0.46(9)$ value is near to the Alaga value of 0.70, the difference indicates band mixing or other effects.

In ^{156}Gd, $B(E2, 0_2{}^+ - 2_g) = 0.15$ e^{2}b^2 (= 30 W.u.) indicates good collectivity. In ^{158}Dy, a $0_g - 2_\beta E2$ strength of about 10 W.u. (table 1) again indicates good collectivity [26].

In the present work for ^{158}Dy, with a slightly larger quadrupole strength parameter X_Q (see sect. 3.1) of DPPQM, we get improved predictions of the γ-g, β-g $E2$

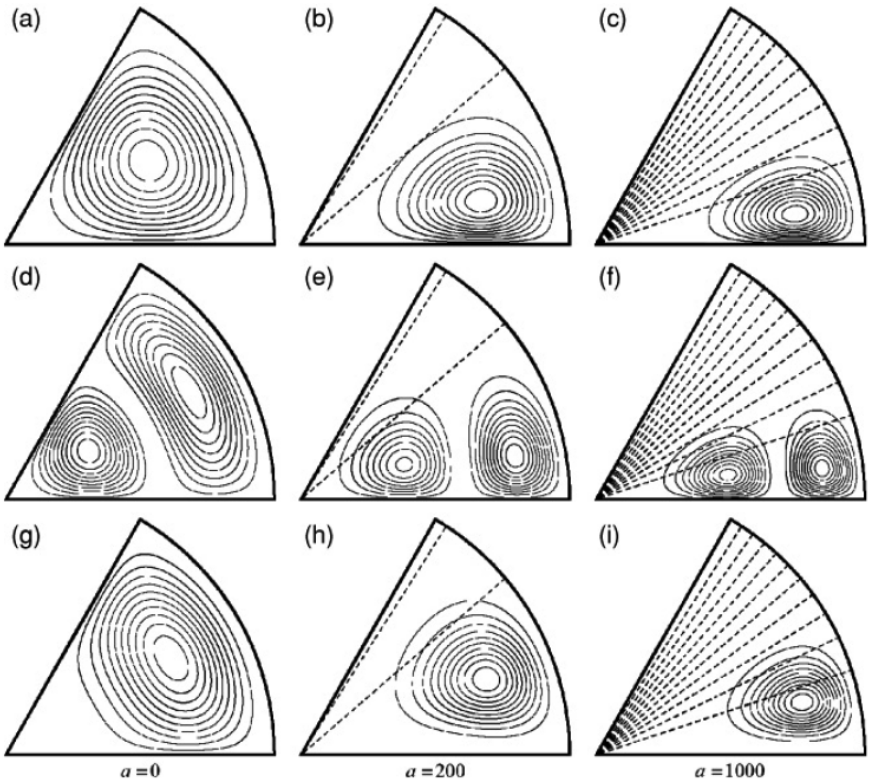

Fig. 16. The probability distributions on the (β, γ) space, from the exact solution of $X(5)$ Hamiltonian. Top row is for ground state, middle for β-band head and bottom for γ-band head. Left column is for γ-stiffness parameter $a = 2AB\beta_w^2/h^2 = 0$ (γ-soft), middle for $a = 200$, and right column for $a = 1000$. The dashed lines represent the potential $V_\gamma(\gamma) = a\gamma^2$ (see [30] for details).

transitions (table 1), than obtained in [26]. In going across $N = 88$–98, at $N = 92$ the character of $I^\pi = 2_2{}^+$ state undergoes a change from the 2_β to 2_γ. The DPPQ model, yields large K-admixtures in the β, γ bands. The predicted $B(E2)$ (small values) are very sensitive to the quadrupole strength parameter X_Q in DPPQM. Hence, the inverted order of the calculated 2_β and 2_γ is retained.

In ^{160}Er there are well developed g-, $K = 2$ and $K = 0_2$ bands. Dusling *et al.* [39] studied it in a confined β-soft (CBS) model and reproduced level energies and $B(E2)$ ratios. By comparison with IBM and $X(5)$ critical symmetry, they ascribed the $K = 0_2$ as a β-band head. In DPPQM strong mixing between $K = 2$ and 0_2 bands is predicted. As in ^{158}Dy, here in ^{160}Er too, the DPPQ model predictions are very sensitive to slight changes in the quadrupole strength X_Q. As an alternative, we have calculated its spectrum in IBM-1, where the level energies are input. Except the $B(E2, 0_2 - 2_\gamma)$, which is most sensitive to parameter variation, all other $B(E2)$s agree reasonably well with DPPQM values (see footnote in table 2).

Next we look at the $N = 94$ isotones of Gd and Dy (table 1). Borner *et al.* [40] did ultra-high-resolution study of ^{158}Gd to obtain absolute $B(E2)$ values associated with $K^\pi = 0_2{}^+, 0_3^+$ (1196, 1453 keV) and $K = 2$ γ-band at 1187 keV, from life time measurements. For the 1407 keV $KI = 0_2 4_3$ state, they deduced $B(E2, 4_3 - 2_\gamma) = 13$ W.u. and $B(E2, 4_3 - 3_\gamma) = 38$ W.u. and weaker $E2$ transitions to the ground band. Due to the close proximity of the $K = 0_2$ and $K = 2$ bands, these values could be reproduced in the 3-band mixing calculation. The previously assigned $E2$ transitions from $KI = 0_3 4_4$ state at 1517 keV to 2_γ, 3_γ were excluded from the decay scheme on the basis of very precise energy measurement. Thus, Borner *et al.* [40] found no evidence for a $\gamma\gamma$ phonon excitation in 0_2 (1196 keV) or 0_3 (1453 keV) states.

The DPPQM value of $B(E2, 4_{02} - 2_{02})$ of 1.11 e^2b^2 falls short of 2.30 obtained in [40]. But the DPPQM value of $B(E2, 2_1{}^+ - 0_1{}^+) = 0.92$ e^2b^2 is consistent with known value of 1.0 e^2b^2. The former value also exceeds $B(E2, 4_1{}^+ - 2_1{}^+)$ by about a factor of 2. The $B(E2, 2_\beta - 0_\beta) = 0.74$ e^2b^2 in DPPQM is slightly lower than the $B(E2, 2_1{}^+ - 0_1{}^+)$ value (fig. 10). We get $R' = B(E2, 0_2{}^+ - 2_\gamma/2_g) = 2.2$ which is within the predictions of band mixing here. Over all, our results are in accord with the data and the adequacy of band mixing [40] in ^{158}Gd.

In ^{160}Dy the $0_2{}^+$ state at 1280 keV lies 300 keV above 2_γ at 966 keV, but no absolute value for $0_2 - 2_\gamma$ is available. Gunther *et al.* [6] from a very low intensity of the 313.6 keV $(0_2 - 2_\gamma)$ transition estimated $B(E2, 0_2 - 2_\gamma)/B(E2, 0_2 - 2_g)$ ratio of < 25 instead of 300 derived from Alaga ratios [5], and excluded the $0_2{}^+ = \gamma\gamma$ possibility. $B(E2, 0_g - 2_\beta)$ of about 4 W.u. is low, as in ^{166,168}Er (fig. 12(a)). In DPPQM we predict larger $B(E2, 0_g - 2_\beta)$ and $B(E2, 0_\beta - 2_g)$ values. Also, $B(E2, 2_\beta - 0_\beta)$ is comparable to $B(E2, 2_g - 0_g)$.

In ^{160}Gd ($N = 96$) the absolute $B(E2) \uparrow$ to 2_β or $0_2 - 2_g$ are not available. In DPPQM the two values were 12 and 10 W.u., respectively [24] and $B(E2, 2_\beta - 0_\beta)$ is almost equal to $B(E2, 2_g - 0_g)$ (table 1, fig. 10), thus qualifying for a β-band interpretation.

3.4.3 ^{162}Dy and ^{164}Dy ($N = 96, 98$)

In ^{162}Dy a low 2_γ at 888 keV and high $E(0_2{}^+)$ at 1400 keV leads to a possibility of $0_2{}^+$ being a 2γ phonon state. Kumar [21,22] argued that at such high energy, the nucleus may find it hard to execute β-vibration. It may be easier to under go asymmetric $\gamma\gamma$-vibration. Zamfir *et al.* [41], by using high-efficiency detectors and much better statistics re-assigned several γ-rays in the spectrum of ^{162}Dy. Using E_γ and I_γ of [41,12], the inter-band $B(E2)$ ratios for this nucleus were calculated as presented in [42].

For γ-g transitions ($K = 2$, $I^\pi = 2^+$ to 6^+ states to the states in ground band) the DPPQ values agree well with experiment. The 1453.8 keV $2_3 = 2_{K=02}$ state decays to $I = 0, 2, 4$ states of the ground band and to 2_γ, 3_γ and 4_γ. The calculated $B(E2)$ ratios for transitions from $2_{K=02}$, $4_g/2_g = 1.44$, $2_\gamma/2_g = 1.7$, $2_\gamma/3_\gamma = 0.30$ and $4_\gamma/3_\gamma = 0.90$. In DPPQM we obtained slightly larger values of 3.2, 7.3, 1.0 and 2.9, respectively [42]. The calculated $K = 2$ component admixture in the $2_{K=02}$ state is only 1.7%.

For the 1400 keV 0_2 state, we obtained $B(E2, 0_2 - 2_\gamma/2_g) = 2.0$ compared to 9.4 ± 5.0 in experiment [41]. Thus the preferential decay of $K = 0_2$ band to $K = 2$ γ-band is supported in our calculation, even if there is not much mixing of the two bands. DPPQ values of $B(E2, 0_\beta - 2_g)$ of 16 W.u. and large $B(E2, 2_\beta - 0_\beta) = 1.19$ e^{2}b^2, equal to $B(E2, 2g - 0_g)$, indicate good collectivity.

At $N = 98$ in ^{164}Dy, the $K = 2$ γ-band lies low at 761 keV and 0_2 lies higher at 1655 keV. Lehmann *et al.* [43], using GRID technique determined the life time of the $2_{3,K=0}$ state at 1716 keV, yielding $B(E2, 2_3 - 3_1) = (0.3 - 5.4)$ W.u. for the 888 keV transition. The value in ECQF method of IBM I is 38 W.u. far above the data. In DPPQM we obtain it equal to 17 W.u. They also adopted the $B(M1, 2_3 \to 2_2)$ in the range of (8–130)$\times !0^{-4} \mu_N{}^2$, from an earlier (1991) conversion coefficient data. The theoretical value in microscopic HSCF model for the $B(M1) = 0.018$, exceeds the maximum estimate of $B(M1)$ for pure $M1$. From this, Lehmann *et al.* excluded the β-band or $\gamma\gamma$ interpretation.

The DPPQ model predicts a 99.9% $K = 0$ purity in 2_2 and 2_3 states. The large $M1$ value adopted in ref. [43] is not given in DPPQM. Our $B(M1, 2_3 - 2_2) = 0.0001$ only. For well-deformed nuclei, large $M1$ in β-g $E2$ transitions are not expected nor found [3]. Here we note that, our $B(E2)$ ratios for γ-g transitions from $I = 2$, 3, 4, 5, and 6 states, assuming pure $E2$, agree well with experiment. DPPQ values for $B(E2, 0_g - 2_\beta)$ and $B(E2, 0_\beta - 2_g) \sim 6$ W.u. support the collective character of the $0_2{}^+$ state.

3.4.4 $^{162\text{-}168}$Er

These are well-deformed nuclei with $0_2{}^+$ above 2_γ As cited in fig. 4, a peak is formed at $N = 98$ in ^{166}Er. Recently,

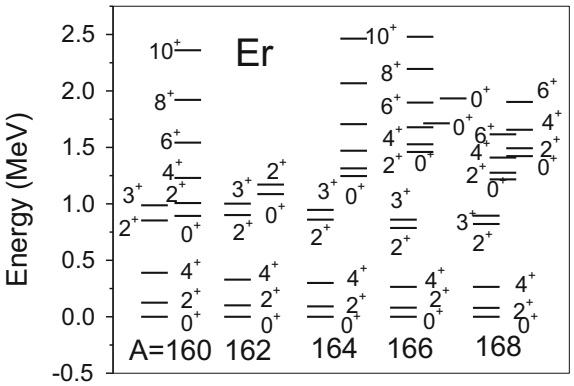

Fig. 17. Partial level scheme of $^{160\text{-}168}$Er. In ^{160,164,166}Er, on $K^\pi = 0_2{}^+$ band head, a rotational band is formed up to $I^\pi = 10^+$.

Caprio *et al.* [44] studied the excited states of ^{162}Er populated in β-decay, in high-statistics coincidences with TRIUMF ISAC facility. The absolute $B(E2)$ strength for excitation of the $0_2{}^+$ 1087 keV state was determined precisely, as also for some other transitions, important to determine the nature of $K^\pi = 0_2{}^+$ band, were measured. The $K = 0_2$ state at 1087 keV along with $2_3{}^+$ at 1171 keV with $B(E2, 0_g - 2_3{}^+)$ of 8 W.u. measured in Coulomb excitation [45], favored it as β-vibration [44]. The DPPQ value (table 2) is higher by a factor of two, and $B(E2, 2_3{}^+ - 0_2{}^+)$ is almost equal to $B(E2, 2_g - 0_g)$ signifying good collectivity.

In ^{164}Er, a rotational band up to $I = 10$ is built on the $0_2{}^+$ 1.246 MeV state (see fig. 17). The E_γ, I_γ values yield the ratio $B(E2, 0_2{}^+ - 2_\gamma/2_g) = 1.92$ indicating mild coupling of $K = 0_2$ and $K = 2$ γ-band. The DPPQM value of 1.05 reflects the same. This is further supported by $B(E2, 2_3 - 2_\gamma/2_g) = 3.10$. The DPPQM value of 0.63 is less. The $B(E2, 0_g - 2_{02})$ of 0.23 (12) W.u. [7] is rather weak and much smaller than the previous value of 1.2 W.u. [12]. DPPQ value of 9 W.u. is much larger. In the DPPQ model calculation, the intra-band $B(E2, 2_3 - 0_2) = 0.98$ e^{2}b^2 is comparable to $B(E2, 2_g - 0_g) = 0.96$ e^{2}b^2. For γ-g transitions in $K = 2$, $I = 2$–6, DPPQ values give excellent agreement with data [12]. Based on its preferred decay to the $K = 2$ band at 800 keV, in DDM [22], the $K^\pi = 0_2{}^+$ at 1246 keV was interpreted as a two phonon $\gamma\gamma$ band. The DPPQM predictions as above indicate the alternative view is equally possible.

In ^{166}Er from the life time data [46] of the 1460 keV 0_2 state, $B(E2, 0_2 - 2_g)$ is 2.5 W.u. For $0_3{}^+$ at 1713, it falls to (0.8–1.6) W.u. but for 0_4 at 1935 keV, it increases to 8.8 W.u., which led to the suggestion that $I = 0_4$ is a β-vibrational state [46]. On the basis of strong 2-neutron transfer strength of the 0_2, 0_3 states, Garrett *et al.* [46] associated them with pairing vibration. Note that no rotational bands have been observed built on the 0_3 and 0_4 states, while there is a rotational band observed built on the $0_2{}^+$ state (up to $I^\pi = 10^+$) (fig. 17).

In DPPQM we predict $B(E2, 2_g - 0_g)$ and $B(E2, 0_g - 2_\gamma)$ in agreement with data (table 2). Also, $R^0_{\gamma g} = B(E2, 0_2 - 2_\gamma)/B(E2, 0_2 - 2_g) \sim 0.9$ agrees with DPPQM

value of 1.4, though each value is twice the observed value (approximately 2 W.u.). In DDM [22], a much larger value for $0_2 - 2_\gamma$ was obtained. Our smaller $B(E2)$, (compared to DDM) coupled with $B(E2, 2_3 - 0_2)$ of 200 W.u. supports collectivity in the $I = 0_2$ state. Our $B(E2, 0_3 - 2_g) = 0.006$ e^2b^2 is essentially equal to the observed value (0.004). But $B(E2, 0_3 - 2_\gamma) = 0.11$ in DPPQM exceeds the experimental value of 0.008 by a factor of 10. Considering the good reproduction of its decay properties in the DPPQ model, $0_2{}^+$ qualifies for a β-band.

In ^{168}Er, the $0_2{}^+$ state at 1217 keV lies much above the 821.0 keV 2_γ state, along with $K = 0_3$, $2_{\beta\gamma}$ and $K = 4_1$ band heads at 1422, 1848, 2056 keV, respectively. In a generalized band mixing calculation, Gunther *et al.* [6] obtained $B(E2)$s for the 1217 keV $K = 0_2 \rightarrow \gamma$ transitions for the $0_2{}^+$ band consistent with data. They excluded the $0_2 = \gamma\gamma$ possibility. The experimental $B(E2, 0_2 - 2_\gamma) = 0.017$ e^2b^2 (4 W.u.) [6] is predicted to be 0.032 in DPPQM [47], 0.095 in IBM and 0.29 e^2b^2 in DDM [22]. Thus our DPPQ value is closer to experiment (within a factor of two).

4 Summary

The level energy systematics of $Z = 60$–72, $N = 84$–104 have been reviewed here. Peaks and valleys are formed by $E(0_2)$ and $E(2_\gamma)$ at different N, for each Z value (figs. 1–4). This indicates the important role of the filling of Nilsson orbitals of neutrons and protons near the Fermi surface, as well as the geometrical entities, the deformation and softness of the nuclear core to axially symmetric and asymmetric vibrations. In an early calculation for predicting the general properties of β-vibrations in rare-earth region, using the quasi-boson approximation and the Nilsson model, Bes [48] predicted the rise of $E(0_2{}^+)$ at $N \geq 92$, and a general rise for more deformed nuclei as in experiment. Bes *et al.* [49] also predicted the peaking of $E(2_\gamma)$ in Dy at $N = 92$–94, as well as the peaking in Er-Yb-Hf at $N = 100$–102, using the same approach.

In fig. 3 we have illustrated a correlation of the energy $E(0_2)$ of the $K = 0_2$ band head and the rotation vibration interaction coefficient "c" in RV formula of ground-state band energies. In fig. 5, a correlation of the band spread of $K = 0_2$ band and $E(2_g)$ is exhibited. A correlation (one-to-one correspondence) of $E(0_2)/E(2_1)$ and the VMI stretching constant "C" is illustrated in fig. 7. Similarly, a correlation of the softness parameter of the $K = 0_2$ band *versus* $R^\beta_{4/2}$ and of the ground-state band *versus* $R_{4/2}$ exists (fig. 8). A similar equality of the $B(E2, 2_\beta - 0_\beta)$ and $B(E2, 2_g - 0_g)$ is exhibited in fig. 10. Except for a few deviations, all the data lie on the diagonal. These systematics support the general picture of the β-vibration bands in most rare-earth nuclei, excluding the pairing vibration or quasi-particle mixture in a sizable way.

Intra-band and inter-band β-g transitions both exhibit varying nuclear structure in agreement with the level energy systematics. The evidence for β-vibrations assigned to $0_2{}^+$ states are presented here in detail. The fact of $B(E2, 2_\beta - 0_g)$ less than $B(E2, 2_\gamma - 0_g)$ is reproduced in IBM as well as in the microscopic theory. The lack of overlap in the wave functions $A_{200}(\beta, \gamma)$ of $0_2{}^+$ and $A_{100}(\beta, \gamma)$ of the ground state and their band members (fig. 14) explains the reduced $B(E2, \beta - g)$ $E2$ transition strength in addition to the $E2$ operator values. In general, IBM-1 predicts weak β-g and strong β-γ $E2$ transitions. In the DPPQ model both of these properties are reproduced, even if deviations from experiment are larger in some cases. In a large number of nuclei, $0_2{}^+$ states are below 2_γ, or almost overlapping, or only slightly higher. As already pointed out in the literature, this excludes a 2γ interpretation. If 2_γ is low and $0_2{}^+$ high, a 2γ $K = 0$, 2, 4 combination is in principle possible, and a larger β-γ strength and a weaker β-g transition is natural. In such cases, one should also look at the $2_{K=02} \rightarrow 0_2{}^+$ and other intra-band transition to examine the collectivity in such well-deformed nuclei (fig. 10). The importance of these facts, even if known previously, are illustrated here for the first time.

JBG appreciates the post retirement association with Ramjas College, University of Delhi. The work at Vanderbilt University is supported by the U.S. Department of Energy under Grant No.DE-FG05-88ER40407.

References

1. A. Bohr, B.R. Mottelson, *The Nuclear Structure*, Vol. **II** (W.A. Benjamin, 1975).
2. F. Iachello, A. Arima, *The Interacting Boson Model* (Cambridge University Press, Cambridge, 1987).
3. J.H. Hamilton, Izv. Akad. Nauk, USSR Ser., Fiz. **36**, 17 (1972).
4. R.F. Casten, P. von Brentano, N.V. Zamfir, Phys. Rev. C **49**, 1840 (1994).
5. R.F. Casten, P. von Brentano, Phys. Rev. C **51**, 3528 (1995).
6. C. Gunther, S. Boehmsdorff, K. Freitag, J. Manns, U. Muller, Phys. Rev. C **54**, 679 (1996).
7. P.E. Garrett, J. Phys. G **27**, R1 (2001).
8. W.-T. Chou, Gh. Cata-Danil, N.V. Zamfir, R.F. Casten, N. Pietralla, Phys. Rev. C **64**, 057301 (2001).
9. N.V. Zamfir, R.F. Casten, M.A. Caprio, C.W. Beausang, R. Krucken, J.R. Novak, J.R. Cooper, Gh. Cata-Danil, C.J. Barton, Phys. Rev. C **60**, 05312 (1999).
10. H. G. Borner, P. Mutti, M. Jentshel, N.V. Zamfir, R.F. Casten, E.A. McCutchan, R. Krucken, Phys. Rev. C **73**, 034314 (2006).
11. S. Hinds *et al.*, Phys. Lett. B **14**, 48 (1965).
12. nndc, `http://www.nndc.bnl.gov/ensdf`.
13. K. Kumar, M. Baranger, Nucl. Phys. A **110**, 529 (1968).
14. J.B. Gupta, Phys. Rev. C **28**, 1929 (1983).
15. F. Iachello, Phys. Rev. Lett. **87**, 052502 (2001).
16. J.B. Gupta, Eur. Phys. J. A **48**, 177 (2012).
17. R.M. Clark, M. Cromaz, M.A. Deleplanque, R.M. Diamond, P. Fallon, A. Görgen, I.Y. Lee, A.O. Macchiavelli, F.S. Stephens, D. Ward, Phys. Rev. C **67**, 041302 (2003).
18. N. Pietralla, O.M. Gorbachenko, Phys. Rev. C **70**, 011304 (2004).

19. M.A.J. Mariscotti, G. Scharff-Goldhaber, B. Buck, Phys. Rev. **178**, 1864 (1969).
20. P. von Brentano, N.V. Zamfir, R.F. Casten, W.G. Rellergert, E.A. McCutchan, Phys. Rev. C **69**, 044314 (2004).
21. K. Kumar, Phys. Rev. C **51**, 3524 (1995).
22. K. Kumar, *Nuclear Models and the Search for Unity in Nuclear Physics* (Universitetsforlaget, Bergen, 1984).
23. D.A. Meyer *et al.*, Phys. Rev. C **74**, 044309 (2006).
24. K. Kumar, J.B. Gupta, Nucl. Phys. A **304**, 295 (1978).
25. J.B. Gupta, Phys. Rev. C **39**, 1604 (1989).
26. J.B. Gupta, J.H. Hamilton, A.V. Ramayya, Nucl. Phys. A **542**, 429 (1992).
27. S. Raman, C.W. Nestor, P. Tikkanen, At. Data Nucl. Data Tables **78**, 1 (2001).
28. R.F. Casten, D.D. Warner, Rev. Mod. Phys. **60**, 389 (1988).
29. J.B. Gupta, K. Kumar, J.H. Hamilton, Phys. Rev. C **16**, 427 (1977).
30. M.A. Caprio, Phys. Rev. C **72**, 054323 (2005).
31. J.B. Gupta, S. Sharma, Ind. J. Pure Appl. Phys. **26**, 601 (1988).
32. K. Kumar, Nucl. Phys. A **234**, 39 (1974).
33. J.B. Gupta, K. Kumar, J.H. Hamilton, Int. J. Mod. Phys. E **19**, 1491 (2010).
34. K. Kumar, J.B. Gupta, J. Phys. G **10**, 525 (1984).
35. R.M. Clark, R.F. Casten, L. Bettermann, R. Winkler, Phys. Rev. C **80**, 011303 (2009).
36. K. Kumar, J.B. Gupta, J.H. Hamilton, Austr. J. Phys. **32**, 307 (1979).
37. J.B. Gupta, *Third International Conference on Fission and Properties of Neutron-Rich Nuclei*, edited by J.H. Hamilton, A.V. Ramayya, H.K. Carter (World Scientific, Singapore, 2003) p. 296.
38. R. Krucken *et al.*, Phys. Lett. B **454**, 15 (1999).
39. K. Dusling *et al.*, Phys. Rev. C **73**, 014317 (2006).
40. H.G. Borner, M. Jentschel, N.V. Zamfir, R.F. Casten, M. Krticka, W. Andrejtscheff, Phys. Rev. C **59**, 2432 (1999).
41. N.V. Zamfir, R.F. Casten, Benyuan Liu, D.S. Brenner, C.J. Barton, R. Krücken, C.W. Beausang, J.R. Novak, J.R. Cooper, G. Cata-Danil, R.L. Gill, D.D. Warner, Phys. Rev. C **60**, 054319 (1999).
42. J.B. Gupta, Nucl. Phys. Symp. (India) **52**, 222 (2007).
43. H. Lehmann, J. Jolie, F. Corminboeuf, H.G. Borner, C. Doll, M. Jentshel, R.F. Casten, N.V. Zamfir, Phys. Rev. C **57**, 569 (1998).
44. M.A. Caprio, R.F. Casten, N.V. Zamfir, G.C. Ball, K.P. Jackson, P.-A. Amaudruz, J.-C. Thomas, Phys. Rev. C **66**, 014307 (2002).
45. R.M. Ronningen, R.S. Grantham, J.H. Hamilton, R.B. Piercey, A.V. Ramayya, B. van Nooijen, H. Kawakami, W. Lourens, R.S. Lee, W.K. Dagenhart, L.L. Riedinger, Phys. Rev. C **26**, 97 (1982).
46. P.E. Garrett, M. Kadi, C.A. McGrath, V. Sorokin, Min Li, Minfang Yeh, S.W. Yates, Phys. Lett. B **400**, 250 (1997).
47. J.B. Gupta, J.H. Hamilton, A.V. Ramayya, Phys. Rev. C **63**, 044308 (1999).
48. D.R. Bes, Nucl. Phys. **49**, 544 (1963).
49. D.R. Bes, P. Federmanm, E. Maqueda, A. Zuker, Nucl. Phys. **65**, 1 (1965).